Talanta 223 (2021) 121719

Contents lists available at ScienceDirect

Talanta

journal homepage: www.elsevier.com/locate/talanta

Ultrasensitive sandwich-like electrochemical biosensor based on core-shell Pt@CeO_2 as signal tags and double molecular recognition for cerebral dopamine detection

Cuiping Fu [a,1], Yina Sun [a,1], Chuan Huang [a,1], Fangfang Wang [a], Na Li [b], Lina Zhang [c,**], Shenguang Ge [a,*], Jinghua Yu [b]

[a] Collaborative Innovation Center of Technology and Equipment for Biological Diagnosis and Therapy in Universities of Shandong, Institute for Advanced Interdisciplinary Research, University of Jinan, Jinan, 250022, PR China
[b] Collaborative Innovation Center for Green Chemical Manufacturing and Accurate Detection, School of Chemistry and Chemical Engineering, University of Jinan, Jinan, 250022, PR China
[c] Shandong Provincial Key Laboratory of Preparation and Measurement of Building Materials, University of Jinan, Jinan, 250022, PR China

ARTICLE INFO

Keywords:
Dopamine
Electrochemical biosensor
Cerium oxide
Double molecular recognition

ABSTRACT

In this report, 4-mercaptophenylboronic acid (MBA) and dithiobis (succinimidyl propionate) (DSP) were used as DA molecular recognizer, which bounded onto the prepared Pt@CeO_2 nanomaterial and the electrode surface. A sandwich-like electrochemical biosensor was constructed for sensitive detection of dopamine (DA) based on double molecular recognition and Pt@CeO_2 (MBA-DSP- Pt@CeO_2) as an electrochemical probe for signal amplification. It is worth noting that the diol and amine groups of DA were reacted by the boronic acid of MBA and the succinimide residue of DSP, respectively. This sandwich-like double molecular interaction can efficiently and accurately identify DA. The uniform Pt@CeO_2 multicore@shell nanospheres as signal tags and signal amplifiers in electrochemical biosensor were synthesized by hydrothermal, which has excellent catalytic activity for H_2O_2. Interestingly, more oxygen vacancies were produced in the lattice structure of CeO_2 doped with Pt, so that the catalytic and redox performance of the obtained Pt@CeO_2 was much better than that of pure CeO_2, thus greatly improving the performance of the proposed sensor. The proposed electrochemical biosensor provided a wide detection range of 2–180 nM and a low detection limit (0.71 nM) by the electrochemical measurement. And it also showed ultra-high sensitivity, accuracy and broad application prospect, which developed a new research method for early clinical diagnosis.

1. Introduction

Dopamine (DA) is a neurotransmitter that is mainly responsible for the brain's lust, sensation, excitement and happiness messages, and is also associated with addiction [1]. Both smoking and drug use can increase the production of dopamine, making addicts happy and excited. Lack of dopamine can make people lose the ability to control their muscles. The normal concentration of dopamine in human blood is 0.2–0.4 μg/mL. When the DA concentration in human plasma is too low, it will cause many diseases, such as: Parkinson's disease [2–4], heart failure, schizophrenia [5,6], abnormal thyroid hormone content, neuromuscular disorders and other diseases. Obviously, the content of DA is closely related to some diseases of human body. Rapid and sensitive detection of DA content has important application value for physiological function research and clinical diagnosis. Over the past 30 years, a variety of analytical methods, such as electrochemical luminescence [7–10], liquid chromatography [11,12], fluorescence [13–15], have been developed for DA detection. However, these methods can't meet the requirement for the rapid and in situ analysis of DA due to time-consuming, complicated sample preparation and complicated instruments. The electrochemical biosensors have received extensive attention due to their advantages such as low-cost, simple process, fast

* Corresponding author.
** Corresponding author.
E-mail addresses: zhanglina818@126.com (L. Zhang), chm_gesg@163.com (S. Ge).
[1] These authors contributed equally to this work.

https://doi.org/10.1016/j.talanta.2020.121719
Received 13 July 2020; Received in revised form 16 September 2020; Accepted 28 September 2020
Available online 30 September 2020

response and high sensitivity [16].

In the case of utilizing electrochemical biosensors, many methods have been made to enhance the sensitivity of electrochemical biosensor for the signal amplification [17]. Nanomaterials [18,19] are considered to improve the efficacy because of their morphology, surface properties and composition, and become one of the commonly used and effective markers for signal amplification [20–22] because of catalytic substrates to promote electron transfer. Metal oxides have a wide range of applications in biosensor owing to its low cost [23], stability, especially unique electrical and catalytic properties [24], which make it a promising material for the manufacture of redox pairs for electrochemical biosensors. Cerium dioxide (CeO_2) plays a vital role in biosensor, due to its outstanding catalytic performance [25], high surface oxygen mobility, anti-inflammatory [26], superior bio-compatibility and high adsorption capability [27]. More importantly, the biological characteristics [28] and unique catalytic properties [29] of CeO_2 nanoparticles are a result of their variable oxidation state and allow the reversible $Ce^{4+} \leftrightarrow Ce^{3+}$. However, the redox signal of CeO_2 detected in neutral mild buffer solutions is too weak to be used as a biosensor probe. To enhance the catalytic performance of cerium dioxide. One promising strategy is the integration of Pt catalysts onto strongly interacting CeO_2. After the introduction of dopants, the oxygen vacancy formation energy can be decreased, resulting in the generation of extra oxygen vacancies [30,31]. Therefore, Pt@CeO_2 [32]has better catalytic properties and improved the catalytic efficiency of H_2O_2 [33], which can further increase the detection signal toward the DA.

While the advantages of biosensors are obvious, the selectivity of some previous sensors for biomolecules containing the same diol is still limited [34]. With the purpose of improving this deficiency, a sandwich-like sensor is developed via bimolecular double recognition, which superbly improved the sensitivity of DA detection. First of all, the substrate of electrodeposited gold nanoparticles binds 4-mercaptophenylboronic acid (MBA) and dithiobis (succinimidyl propionate) (DSP) through Au–S bonds [35], which can promote electron transfer, achieve the improvement of electrode surface conductivity and provide plentiful sites for capture DA molecules. Meanwhile, Pt@CeO_2 nanomaterial also binds MBA and DSP, which can not only identify DA but also be used as the signal tags for signal amplification. In this sensor, both MBA and DSP specifically bind to DA through chemical bonds. Therefore, the combination of bimolecular recognition and sandwich sensors can detect DA with higher sensitivity and selectivity at the nanometer level. The chemical structure diagram of the chemical reaction of dopamine with MBA and DSP was shown in Fig. S1 of the Supporting Material.

In this study, an ultrasensitive electrochemical sandwich-like biosensor was fabricated for detection of DA based on MBA and DSP double molecular recognition. As shown in Scheme 1, Pt@CeO_2 was modified with MBA and DSP to form MBA-DSP-Pt@CeO_2 probe. At the same time, MBA and DSP were also combined on the glassy carbon electrode modified gold nanoparticles [34] by electrodeposition through Au–S bond. In the presence of target DA, boronic acid in MBA formed stable boronated complexes with diols of DA, while the amine-reactive succinimidyl residue in DSP reacted with the amine groups of DA. These two molecules were modified on both sides of the sensor, which interacted with diols and amine functional groups of DA, respectively, doubly recognized DA with high specificity [36]. Since Pt was doped into CeO_2 lattice structure, endowing Pt@CeO_2 with a superior catalytic activity. As a result, the electrochemical signal was largely amplified in the presence of H_2O_2 due to the high catalytic activity of Pt@CeO_2 toward H_2O_2. The Pt@CeO_2 current signal was used to reflect the concentration of DA. Most importantly, the proposed biosensor provides a feasible method for DA detection by bimolecular recognition, which shows a promising platform for clinical application.

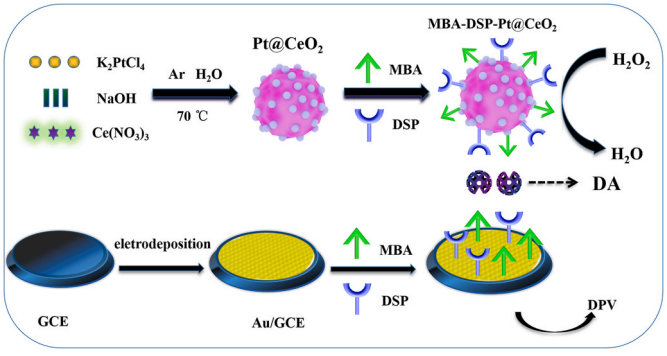

Scheme 1. Schematic of sandwich-like electrochemical biosensor for detection of DA.

2. Experimental

2.1. Materials and apparatus

The materials and apparatus are described in the Supplementary Material.

2.2. Preparation of Pt@CeO_2 core-shell nanospheres

The whole synthetic process was performed under Ar gas protection. An aliquot of 1 mL of 0.1 M $Ce(NO_3)_3$ was added to 10 mL of H_2O, and then Ar gas was bubbled into the solution for 10 min. Then, 1 mL of 0.2 M NaOH aqueous solution was rapidly added, followed immediately by the quick addition of 1 mL of 0.01 M K_2PtCl_4. The solution was heated at 70 °C for 1 h. After being cooled to room temperature, the sample was purified by centrifugation to remove the residual K_2PtCl_4 solution, which remained in the supernatant solution [37]. Finally, the as-obtained samples were directly dried at 80 °C overnight.

2.3. Preparation of MBA-DSP-Pt@CeO_2 probe

Modification of Pt@CeO_2 was performed at room temperature by mixing 6 mL of the as-prepared Pt@CeO_2 with 20 μL of aqueous solution of 1 mM MBA and 2 mM DSP, and then placed the mixed solution on a shaker overnight.

2.4. Fabrication of the sensor

The whole preparation process of the sensor was shown in Scheme 1. Typically, this process could be summarized in five steps: (1) Treatment of bare electrodes. The bare GCE was polished with an alumina slurry. Thereafter, the bare GCE was subjected to ultrasonic treatment in methanol and ultrapure water, followed by electrochemical pretreatment, and potential cycling was performed in a solution of potassium ferricyanide solution, ranging from −0.2 to +0.6 V. The scan rate was 100 mV/s until a stable cyclic voltammogram was observed. Finally, the bare GCE was rinsed with a large amount of ultrapure water and dried. (2) Electrochemical deposition of gold nanoparticles. The treated GCE was placed in a 1% $HAuCl_4$ solution with a deposition potential of −0.2 V and a deposition time of 60 s (3) An aliquot of 10 μL of 2 mM MBA and 10 μL of 4 mM DSP were dropped on the surface of the electrode treated in the step (2), and reacted at room temperature for 6 h; (4) Adding a certain concentration of dopamine solution to the surface of the prepared electrode in the step (3), and standing at room temperature for 5 min, the electrode was cleaned by ultrapure water; (5) 20 μL of MBA-DSP-Pt@CeO_2 nanoparticle composite was added dropwise to the surface of the electrode treated in step (4), and left at room temperature for 5 min, and the electrode was washed with ultrapure water. The electrode was dipped into pH 7.4 0.01 M PBS buffer solution containing 1 mM hydrogen peroxide. CV and differential pulse voltammetry (DPV) measurements were conducted from −0.5 to +0.2 V with the scan rate of 50 mV/s.

2.5. Simulated sample preparation

5 mM ascorbic acid, 5 mM glucose, 500 nM 3,4-dihydroxyphenylacetic acid, 20 nM epinephrine, 20 nM norepinephrine, 5 mM Lactate were added to 0.01 M PBS buffer solution. A certain amount of DA was added to the above solution for detection.

3. Results and discussions

3.1. Characterization of materials

To verify the shape and formation of Pt@CeO_2, the morphologies of Pt@CeO_2 nanocomposites were characterized by SEM. As shown in Fig. 1A, the Pt@CeO_2 showed uniform-size nanospheres and a rough surface of the nanosphere was observed from the SEM image. The EDS mapping images (Fig. 1B) revealed the occurrence of homogeneous distributions of Ce, Pt and O. Moreover, the element peaks of Ce, Pt and O, in energy dispersive spectroscopy (EDS) analysis (Fig. 1C) confirmed the formation of Pt@CeO_2 nanocomposites. Further, TEM was applied to investigate their morphologies (Fig. 1D), the characteristic of TEM were consistent with the corresponding SEM image and the size of Pt@CeO_2 nanocomposites about 72 nm.

The composition and electronic structure of the Pt@CeO_2 NPs was further confirmed to the analysis of Pt_{4f}, Ce_{3d} and O_{1s} by x-ray photoelectron spectroscopy (XPS). XPS spectra of the resulting Pt@CeO_2 showed significant Pt_{4f} signals corresponding to the binding energy of Pt. In Fig. 2A, the major peaks at 72.8 eV and 76.2 eV can be assigned to the $4f_{7/2}$ and $4f_{5/2}$ Pt metal states. The Ce ($3d_{3/2}$, $3d_{5/2}$) peaks at 882.6 eV and 898.3 eV with characteristic sites (marked in Fig. 2B) correspond to CeO_2 with Ce in the +4 oxidation state. And as shown in Fig. 2C, the O (1s) peak is observed at 285 eV in the as-prepared sample, which corresponds to CeO_2. These results supported the conclusion that Pt@CeO_2 hybrid nanomaterials had been successfully synthesized. To verify the formation of Pt@CeO_2, an X-ray diffraction (XRD) technique was conducted. As shown in Fig. 2D, the synthesized Pt@CeO_2 displays sharp diffraction peaks in XRD patterns, which are highly consistent with the simulated data from the single crystal, implying good purity and high crystallinity. No characteristic peaks from other impurities are detected, indicating the high purity of the as-synthesized Pt@CeO_2 nanospheres.

3.2. Verification of the sensing strategy

The immobilization of MBA and DSP on the Pt@CeO_2 was confirmed by the Infrared spectra (IR) analysis. As shown in Fig. 3A, the stretching vibration of the infrared spectra at B (1500 cm^{-1}) and D (2849 cm^{-1}) is caused by the C═C and C–H of the benzene ring, which proves the existence of the benzene ring. The peak value at A (705 cm^{-1}) belongs to the stretching vibration of C–S. The stretching vibration of the infrared spectra at C (1718 cm^{-1}) and E (3489 cm^{-1}) is caused by the C═O and O–H of the benzene ring, which proves the existence of the carbonyl and hydroxyl groups. These characteristics indicate that MBA and DSP molecules are successfully modified at the surface of Pt@CeO_2 nanoparticles.

Signal amplification is critical for a sandwich-type electrochemical bioanalysis. In order to investigate the signal amplification effect of Pt doped CeO_2 composite nanomaterials on the detection of dopamine, three differently labeled probes were prepared: CeO_2-bound MBA-DSP, PtNPs-bound MBA-DSP and Pt@CeO_2 combined MBA-DSP. During the measurement process, the same concentration of DA was dropped on the modified electrode of the same batch, and then variously labeled probes were used to detect dopamine by cyclic voltammetry. This judgment was

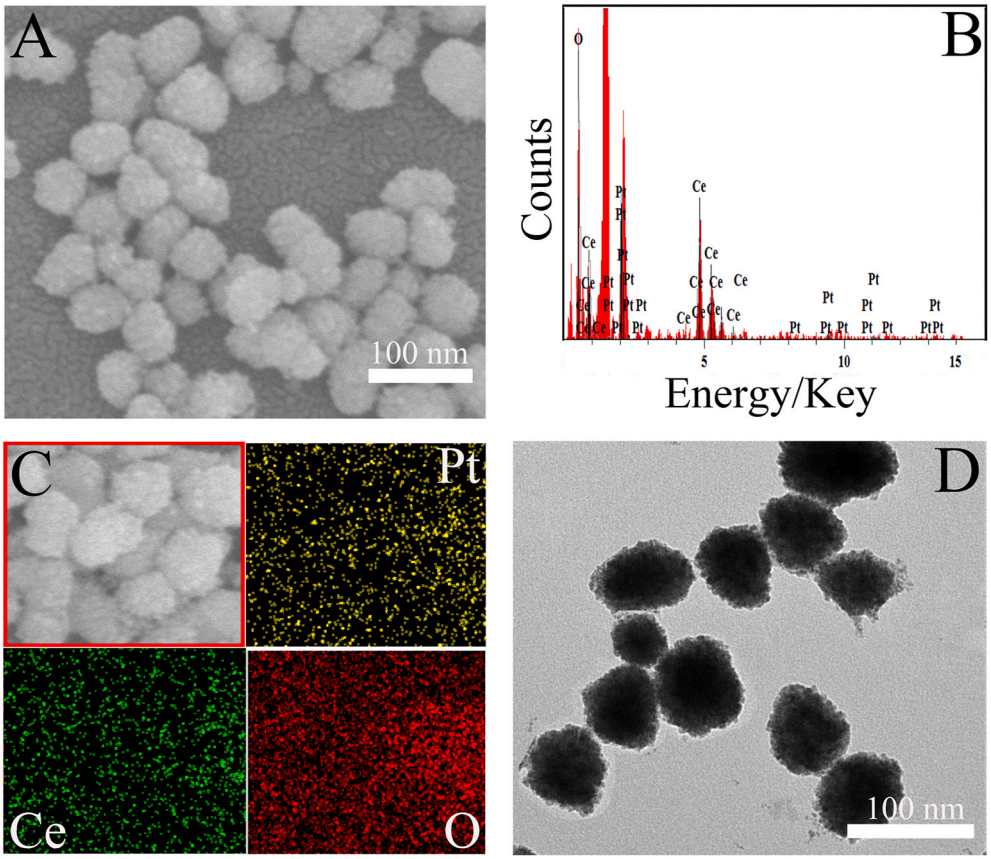

Fig. 1. SEM image of the Pt@CeO_2 (A), EDS patterns of the Pt@CeO_2 nanospheres (B), EDS mapping images of Pt (yellow), Ce (green), and O (red) (C), TEM image of the Pt@CeO_2 (D). (For interpretation of the references to colour in this figure legend, the reader is referred to the Web version of this article.)

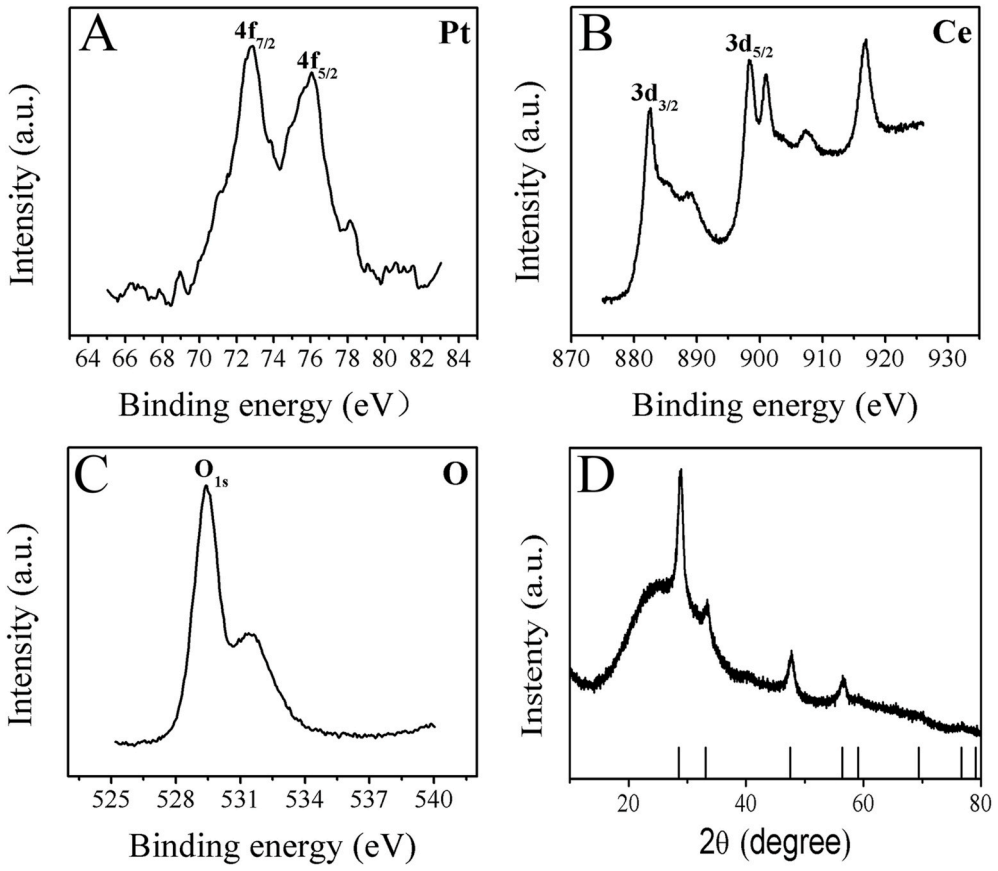

Fig. 2. XPS spectra of (A) element Pt; (B) element Ce; (C) element O. (D) XRD patterns of Pt@CeO_2 nanospheres.

based on the change in amperage of the sensor with different probes. As shown in Fig. 3B, Pt@CeO_2-MBA-DSP exhibited much greater current than those obtained at other two labeled probes. The reason is that doping Pt in the lattice of CeO_2 increases the oxygen vacancy, which the Pt@CeO_2 has better redox ability. Therefore, the Pt@CeO_2-MBA-DSP probe was chosen for the following experiments.

In order to study the effect of double connection between MBA and DSP on the detection of dopamine, a set of comparative experiment was carried out, (a) MBA-DSP was modified on AuNPs/GCE and Pt@CeO_2 respectively, (b) MBA was modified on AuNPs/GCE, DSP was connected with Pt@CeO_2, (c) DSP was modified on AuNPs/GCE, MBA was connected with Pt@CeO_2. During the measurement process, the same concentration of DA was dripped to the different modified electrodes, and then decorated with DSP-Pt@CeO_2, MBA-Pt@CeO_2 and MBA-DSP-Pt@CeO_2 respectively. The change of the current signal of DPV was used to judge the influence of different sensors connected by MBA and DSP on the detection of dopamine. As shown in Fig. 3C, the response of DPV modified with both MBA and DSP on both sides of the sensor was larger than that of single MBA or DSP respectively. Therefore, the co-modification of MBA and DSP was more superior than that of the single modification of MBA or DSP, and the signal was strong. So, MBA and DSP were chosen to modify the electrode and the Pt@CeO_2 for the next experiments.

Different ratios of MBA and DSP were anchored to the Pt@CeO_2 nanocomposites and the modified electrode for 60 nM dopamine detection. As shown in Fig. 3D, the optimum concentration ratio of MBA to DSP is 1/2.

3.3. Effect of experimental conditions

In the prepared sandwich sensor, the pH of the detection solution and the concentration of H_2O_2 influenced the electrochemical signal. The pH of the detection solution will affect the activity of dopamine. Since H_2O_2 catalyzed oxidation by Pt@CeO_2 can accelerate electron transfer from Ce^{3+} to Ce^{4+}, H_2O_2 concentration played an important role on performance of signal amplification. As shown in Fig. S1A and Fig. S1B, it was obvious that the pH 7.4 PBS buffer solution and 1 mM H_2O_2 were the best choice for this biosensor. (Detailed description of Fig. S2A and Fig. S2B see the Supplementary Material).

3.4. Electrochemical behavior of the biosensor

The properties of the electrode at each step are investigated by CV (+0.6 to −0.2 V with the scan rate of 50 mV/s). CV measurements were constructed in 5.0 mM of $[Fe(CN)_6]^{3-/4-}$ solution containing 0.1 M KCl. The experimental results were shown in Fig. 4A. The bare GCE (Fig. 4A curve a) had a good redox peak in $[Fe(CN)_6]^{3-/4-}$ solution. When AuNPs was electrodeposited on the electrode surface (Au/GCE, Fig. 4A curve b), the redox peak current increased obviously, which proved that AuNPs had good conductivity and large surface area. After the MBA and DSP were fixed on the surface of Au/GCE, the peak current was decreased (Fig. 4A curve c). The reason was that the modification of organic molecules reduced the electrode surface area and hindered $[Fe(CN)_6]^{3-/4-}$ from reaching the electrode surface, thus reducing the peak current. Then continued to load DA on the electrode surface, the peak current continued to decrease (Fig. 4A curve d). When Pt@CeO_2 was introduced into the electrode surface, it affected the redox of Fe^{2+} and Fe^{3+}, increased the steric hindrance, and showed the decrease of peak current and the increase of redox potential difference on the CV diagram (Fig. 4A curve e).

Electrochemical impedance spectroscopy (EIS) is an effective tool to characterize the interface characteristics of the modified electrode. Fig. 4B showed the AC impedance diagrams of different modified electrodes in 5.0 mM of $[Fe(CN)_6]^{3-/4-}$ solution containing 0.1 M KCl. The

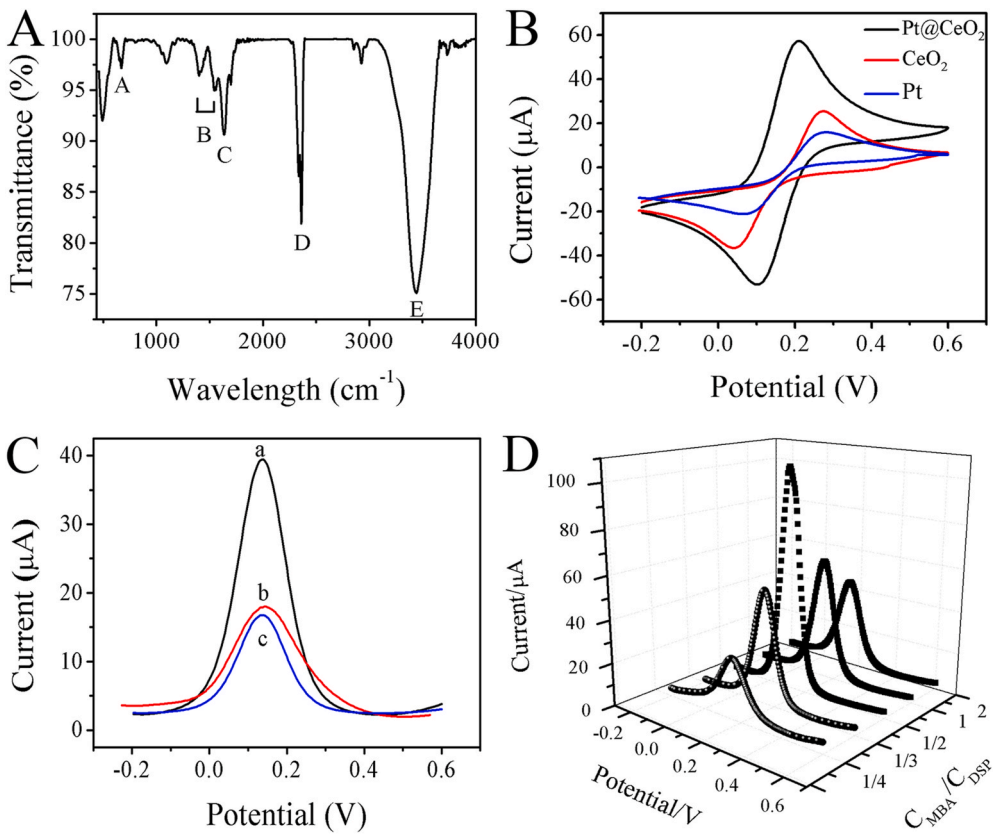

Fig. 3. (A) IR spectra of the MBA-DSP-Pt@CeO_2 probe. (B) CV of the various probe nanomaterials Pt@CeO_2, CeO_2, and Pt modified to probe. (C) Signal intensity variation of the Pt@CeO_2 functionalized by different concentration ratios of MBA and DSP toward the addition of 160 nM DA. (D) DPV response of the MBA and DSP modified the sensor separately or jointly.

charge-transfer resistance (Ret) was significantly different in the impedance diagrams of different modified electrodes. The bare GCE has a smaller resistance (Ret) to show a semicircle (Fig. 4B curve a). However, the R_{et} value decreased significantly after the electrodeposition of AuNPs on GCE (Fig. 4B curve b), indicating that the conductivity of AuNPs accelerated the electron transfer on the electrode surface to a certain extent. When MBA and DSP were fixed to the Au/GCE surface, the R_{et} value increased (Fig. 4B curve c). As a small organic molecule modified on the electrode, DA could hinder the electron exchange between the redox probe and the electrode and further increase the Ret (Fig. 4B curve d). After modified the MBA-DSP- Pt@CeO_2 probe on the electrode, the R_{et} value also increased (Fig. 4B curve e), indicating that the MBA-DSP- Pt@CeO_2 probe successfully connected to the surface of the DA modified electrode. The equivalent circuit provided the value of the cambium on the electrode surface (Supplementary Material Table S1). According to the experimental results, it could be seen that the change of R_{et} value was consistent with that of CV current, indicating that the sensor was successfully designed.

3.5. Analytical performance

Under optimized experimental conditions (see Fig. S1 and Supplementary Material Fig. S1), the electrochemical detection of DA was carried out by the DPV method on the biosensor. The glassy carbon electrode modified with MBA-DSP-AuNPs was dripped with different concentrations of DA, and finally dripped with the same concentration of MBA-DSP-Pt@CeO_2 at room temperature for 5 min and washed thoroughly with secondary water. DPV experiments were carried out in pH 7.4 0.01 M PBS buffer solution containing 1 mM hydrogen peroxide (pulse width, 50 ms; amplitude, 50 mV; sample width, 16.7 ms; pulse period, 200 ms). The result was shown in Fig. 4C, the change of response current increased with the increase of DA concentration. It could be seen from the working curve (Fig. 4D) that there was a good linear relationship between the change of response current and the concentration of analyte in the range of 2–180 nM concentration of DA. The current signal was proportional to the concentration of DA. The biosensor exhibited a linear detection range from 2 nM to 180 nM and the limit of detection (S/N = 3) of 0.71 nM. As shown in Fig. 4D, the linear equation was $I = 8.7619 + 0.5489C$ ($R^2 = 0.9936$) which verified the conclusion drawn from the DPV experiment. The result revealed that the proposed biosensor could provide a wide detection range and an ultrasensitive detection limit toward DA. The detection limit is better than most of the reported research results for quantitative determination of DA (Table S2). These results confirmed enhanced signal amplification effects from the Pt@CeO_2 composites.

3.6. Stability, reproducibility and selectivity of the DA biosensor

The stability is an important parameter to evaluate the characteristics of biosensor. The proposed sensing electrodes were fabricated in the same conditions and stored at room temperature (0, 10, 30, 60, 90 days). The results showed that the current response remained at 89.7% of its original response within 90 days (Fig. 5A). Therefore, the prepared biosensor had satisfactory stability for the detection of DA.

As shown in Fig. 5B, there were no obvious changes for during five consecutive DPV scans, indicating that the repeatability of Pt@CeO_2 signals were exciting. The reproducibility of the sensor was studied as follows. The reproducibility was assessed toward the same concentration of DA solution (160 nM). The experimental data indicated that the relative standard deviation (RSD) values of intra-assays biosensor with five parallel determinations were 3.2%, whereas the RSD values of the inter-assays biosensor with five biosensors were 4.8%. The results

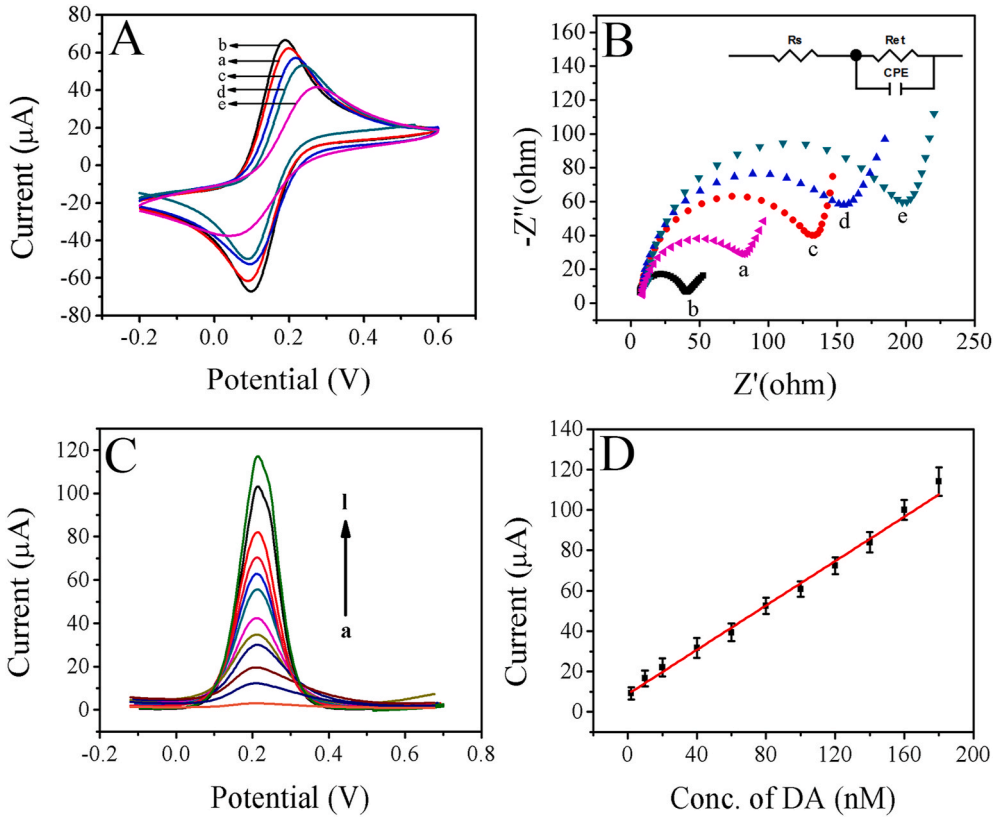

Fig. 4. (A) CV and (B) EIS of (a) bare GCE, (b) Au-GCE, (c) MBA-DSP/Au-GCE, (d) MBA-DSP-Pt@CeO_2, (e) MBA-DSP-Pt@CeO_2/MBA-DSP-Pt@CeO_2 in 5.0 mM of [Fe$(CN)_6]^{3-/4-}$ solution containing 0.1 M KCl. (C) DPV responses to different DA concentrations (a–l: 0, 2, 10, 20, 40, 60, 80, 100, 120, 140, 160, 180 nM) in 0.01 M PBS solution containing 1 mM H_2O_2. (D) Calibration curves for analysis DA.

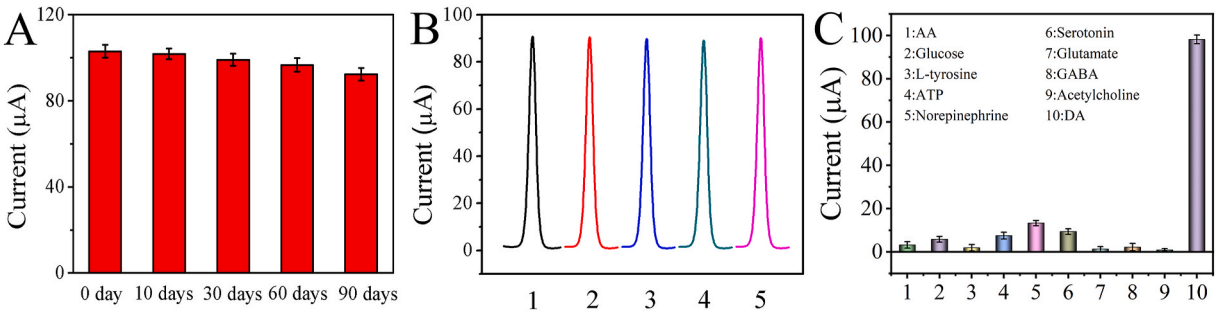

Fig. 5. (A) The storage stability of the biosensor at room temperature. (B) DPV responses of the biosensor for five-time continuous DPV scanning. (C) Selectivity investigation of the proposed sensor for AA, glucose, L-tyrosine, ATP, Norepinephrine, Serotonin, Glutamate, Gamma-Aminobutyric acid (GABA), Acetylcholine, DA in 0.01 M PBS solution containing 1 mM H_2O_2.

demonstrated a good reproducibility of the sensor.

Specificity is significant for the property of the sensor. The complexity of human brain systems brings a huge challenge to the detection of DA. The selectivity of the sensor is studied by comparing the interferers that are common in the brain, such as AA, glucose, L-tyrosine, ATP, Norepinephrine, Serotonin, Glutamate, Gamma-Aminobutyric acid (GABA), Acetylcholine. It could be seen from Fig. 5C that the strongest current signal was observed in the presence of 160 nM of DA, While the response current remained unchanged when tenfold higher concentrations of interfering substances. Compared to target molecule, low responses of the above compounds were observed, thus suggesting high selectivity of the present method.

3.7. Real sample analysis

In order to verify the reliability of the sensor in practical application, the content of DA in the simulated environment of the brain system was continuously monitored. The recovery experiment was carried with the standard addition method. Meanwhile, high-performance liquid chromatography with an electrochemical detector (HPLC-EC) was also employed to determine the simulated samples. As shown in Table 1, the recovery rate of standard addition recovery experiment was between 88.72% and 108.5% within the acceptable range. Meanwhile, the results obtained with the proposed method were in agreement with those obtained by the HPLC-EC, indicating that the sensor had a certain practical value in clinical diagnosis.

Table 1
DA concentration in real samples tested by the developed biosensor.

Sample	Added (nM)	Found (nM)	Recovery %	HPLC-EC (nM)
1	20	17.82	89.1	18.54
2	30	27.47	91.56	29.03
3	40	42.12	105.3	39.91
4	50	44.36	88.72	45.93
5	60	65.08	108.5	63.76

4. Conclusions

In summary, a low-cost, easy to use, high selectivity sandwich-like biosensor was successfully developed for ultrasensitive detection of DA based on double molecular recognition. This biosensor has many positive features: first, the MBA-DSP-Pt@CeO_2 probe can interact with diols and amine functional groups in DA to realize the double recognition of DA. Second, Pt@CeO_2 nanomaterial as a catalyst could catalyze the reduction of H_2O_2 for signal amplification. Third, this method is simple and the requirements for technology and instruments are low. Moreover, compared to other biosensors, the biosensor has better reproducibility, specificity, stability and lower detection limit, which providing a promising platform for point-of-care testing in clinical applications. Nevertheless, the designed biosensor cannot detect multiple analytes simultaneously. In order to break through this limitation, we will find a considerable method that can detect multiple targets on the analysis equipment at the same time in our future work.

Credit author statement

Cuiping Fu, Conceptualization, Methodology, Data curation, Writing - original draft. Yina Sun, Resources, Visualization, Data curation. Chuan Huang, Investigation, Formal analysis. Fangfang Wang, Resources, Visualization. Na Li, Resources, Visualization., Lina Zhang, Writing-Reviewing and Editing, Resources. Shenguang Ge, Conceptualization, Supervision, Funding acquisition. Jinghua Yu, Funding acquisition, Project administration.

Declaration of competing interest

The authors declare that they have no known competing financial interests or personal relationships that could have appeared to influence the work reported in this paper.

Acknowledgements

This work was supported by the National Natural Science Foundation of China (22074053, 21775055, 21874055); A project of Shandong Province Higher Educational Youth Innovation Science and Technology Program (2019KJC016); The Project of “20 items of University” of Jinan (2018GXRC001); the Taishan Scholars program and Case-by-Case Project for Top Outstanding Talents of Jinan.

Appendix A. Supplementary data

Supplementary data to this article can be found online at https://doi.org/10.1016/j.talanta.2020.121719.

References

[1] J.D. Berke, What does dopamine mean? Nat. Neurosci. 21 (6) (2018) 787–793.
[2] I. Badillo-Ramirez, J.M. Saniger, S. Rivas-Arancibia, 5-S-cysteinyl-dopamine, a neurotoxic endogenous metabolite of dopamine: implications for Parkinson’s disease, Neurochem. Int. 129 (2019) 104514.
[3] M. Perez de la Mora, C. Hernandez-Mondragon, M. Crespo-Ramirez, J. Rejon-Orantes, D.O. Borroto-Escuela, K. Fuxe, Conventional and novel pharmacological approaches to treat dopamine-related disorders: focus on Parkinson’s disease and schizophrenia, Neuroscience 439 (2019) 309–318.
[4] M.M. Mokhles, G. Trifiro, J.P. Dieleman, M.D. Haag, E.M. van Soest, K. M. Verhamme, G. Mazzaglia, R. Herings, C. Luise, D. Ross, G. Brusselle, A. Colao, W. Haverkamp, R. Schade, G. Camp, R. Zanettini, M.C. Sturkenboom, The risk of new onset heart failure associated with dopamine agonist use in Parkinson’s disease, Pharmacol. Res. 65 (3) (2012) 358–364.
[5] A. Rakovska, D. Javitt, P. Petkova-Kirova, A. Balla, R. Ang, R. Kalfin, Neurochemical evidence that cysteamine modulates amphetamine-induced dopaminergic neuronal activity in striatum by decreasing dopamine release: an in vivo microdialysis study in freely moving rats, Brain Res. Bull. 153 (2019) 39–46.
[6] G. Zanatta, G. Nunes, E.M. Bezerra, R.F. da Costa, A. Martins, E.W. Caetano, V. N. Freire, C. Gottfried, Antipsychotic haloperidol binding to the human dopamine D3 receptor: beyond docking through QM/MM refinement toward the design of improved schizophrenia medicines, ACS Chem. Neurosci. 5 (10) (2014) 1041–1054.
[7] Y. Gu, J. Wang, H. Shi, M. Pan, B. Liu, G. Fang, S. Wang, Electrochemiluminescence sensor based on upconversion nanoparticles and oligoaniline-crosslinked gold nanoparticles imprinting recognition sites for the determination of dopamine, Biosens. Bioelectron. 128 (2019) 129–136.
[8] L. Li, H. Liu, Y. Shen, J. Zhang, J.J. Zhu, Electrogenerated chemiluminescence of Au nanoclusters for the detection of dopamine, Anal. Chem. 83 (3) (2011) 661–665.
[9] L. Zhang, Y. Cheng, J. Lei, Y. Liu, Q. Hao, H. Ju, Stepwise chemical reaction strategy for highly sensitive electrochemiluminescent detection of dopamine, Anal. Chem. 85 (16) (2013) 8001–8007.
[10] H. Peng, P. Liu, W. Wu, W. Chen, X. Meng, X. Lin, A. Liu, Facile electrochemiluminescence sensing platform based on water-soluble tungsten oxide quantum dots for ultrasensitive detection of dopamine released by cells, Anal. Chim. Acta 1065 (2019) 21–28.
[11] H. Gu, E.L. Varner, S.R. Groskreutz, A.C. Michael, S.G. Weber, In vivo monitoring of dopamine by microdialysis with 1 min temporal resolution using online capillary liquid chromatography with electrochemical detection, Anal. Chem. 87 (12) (2015) 6088–6094.
[12] N.J. Reinhoud, H.J. Brouwer, L.M. van Heerwaarden, G.A. Korte-Bouws, Analysis of glutamate, GABA, noradrenaline, dopamine, serotonin, and metabolites using microbore UHPLC with electrochemical detection, ACS Chem. Neurosci. 4 (5) (2013) 888–894.
[13] Y.-S. He, C.-G. Pan, H.-X. Cao, M.-Z. Yue, L. Wang, G.-X. Liang, Highly sensitive and selective dual-emission ratiometric fluorescence detection of dopamine based on carbon dots-gold nanoclusters hybrid, Sensor. Actuator. B Chem. 265 (2018) 371–377.
[14] J. Jana, J.S. Chung, S.H. Hur, ZnO-associated carbon dot-based fluorescent assay for sensitive and selective dopamine detection, ACS Omega 4 (16) (2019) 17031–17038.
[15] X. Wei, Z. Zhang, Z. Wang, A simple dopamine detection method based on fluorescence analysis and dopamine polymerization, Microchem. J. 145 (2019) 55–58.
[16] B.-R. Li, Y.-J. Hsieh, Y.-X. Chen, Y.-T. Chung, C.-Y. Pan, Y.-T. Chen, An ultrasensitive nanowire-transistor biosensor for detecting dopamine release from living PC12 cells under hypoxic stimulation, J. Am. Chem. Soc. 135 (43) (2013) 16034–16037.
[17] Y. Liang, C. Wu, G. Figueroa-Miranda, A. Offenhausser, D. Mayer, Amplification of aptamer sensor signals by four orders of magnitude via interdigitated organic electrochemical transistors, Biosens. Bioelectron. 144 (2019) 111668.
[18] Y. Sun, M. Luo, X. Meng, J. Xiang, L. Wang, Q. Ren, S. Guo, Graphene/intermetallic PtPb nanoplates composites for boosting electrochemical detection of H_2O_2 released from cells, Anal. Chem. 89 (6) (2017) 3761–3767.
[19] X. Li, B. Liu, X. Hun, Bimetallic nanomaterials as nanocatalysts and the carrier coupling chemiluminescence aptamer strategy for cancer cell detection, Sensor. Actuator. B Chem. 277 (2018) 510–516.
[20] M.F. Wu, Y. Wang, S. Li, X.X. Dong, J.Y. Yang, Y.D. Shen, H. Wang, Y.M. Sun, H. T. Lei, Z.L. Xu, Ultrasensitive immunosensor for acrylamide based on chitosan/SnO2-SiC hollow sphere nanochains/gold nanomaterial as signal amplification, Anal. Chim. Acta 1049 (2019) 188–195.
[21] Z. Chen, G. Lai, S. Liu, A. Yu, Ultrasensitive electrochemical aptasensing of kanamycin antibiotic by enzymatic signal amplification with a horseradish peroxidase-functionalized gold nanoprobe, Sensor. Actuator. B Chem. 273 (2018) 1762–1767.
[22] R. Wang, L. Wang, X. Xu, W. Jiang, An enzyme-free and label-free fluorescence biosensor for microRNA detection based on cascade amplification of DNAzyme-powered three-dimensional DNA walker and hybridization chain reaction, Sensor. Actuator. B Chem. 268 (2018) 287–292.
[23] M. Al-Hashem, S. Akbar, P. Morris, Role of oxygen vacancies in nanostructured metal-oxide gas sensors: a review, Sens. Actuators, B 301 (2019).
[24] W. Jeon, I.-H. Choi, J.-Y. Park, J.-S. Lee, K.-R. Hwang, Alkaline wet oxidation of lignin over Cu-Mn mixed oxide catalysts for production of vanillin, Catal. Today 352 (2019) 95–103.
[25] Y. Li, Y. Zhang, F. Li, J. Feng, M. Li, L. Chen, Y. Dong, Ultrasensitive electrochemical immunosensor for quantitative detection of SCCA using Co_3O_4@CeO_2-Au@Pt nanocomposite as enzyme-mimetic labels, Biosens. Bioelectron. 92 (2017) 33–39.
[26] D. Jampaiah, T. Srinivasa Reddy, A.E. Kandjani, P.R. Selvakannan, Y.M. Sabri, V. E. Coyle, R. Shukla, S.K. Bhargava, Fe-doped CeO_2 nanorods for enhanced peroxidase-like activity and their application towards glucose detection, J. Mater. Chem. B 4 (22) (2016) 3874–3885.
[27] T. Mitsudome, M. Yamamoto, Z. Maeno, T. Mizugaki, K. Jitsukawa, K. Kaneda, One-step synthesis of core-gold/shell-ceria nanomaterial and its catalysis for highly

selective semihydrogenation of alkynes, J. Am. Chem. Soc. 137 (42) (2015) 13452–13455.
[28] P.S. Murphin Kumar, S. Thiripuranthagan, T. Imai, G. Kumar, A. Pugazhendhi, S. R. Vijayan, R. Esparza, H. Abe, S.K. Krishnan, Pt nanoparticles supported on mesoporous CeO_2 nanostructures obtained through green approach for efficient catalytic performance toward ethanol electro-oxidation, ACS Sustain. Chem. Eng. 5 (12) (2017) 11290–11299.
[29] Y. Long, S. Song, J. Li, L. Wu, Q. Wang, Y. Liu, R. Jin, H. Zhang, Pt/CeO_2@MOF Core@Shell nanoreactor for selective hydrogenation of furfural via the channel screening effect, ACS Catal. 8 (9) (2018) 8506–8512.
[30] J. Liu, Z. Dou, T.-a. Zhang, Preparation of oxygen vacancy-controllable CeO_2 by electrotransformation of a CeCl3 solution and its oxidation mechanism, Ceram. Int. 46 (5) (2020) 5976–5982.
[31] Z.H. Yang, S. Ren, Y. Zhuo, R. Yuan, Y.Q. Chai, Cu/Mn double-doped CeO_2 nanocomposites as signal tags and signal amplifiers for sensitive electrochemical detection of procalcitonin, Anal. Chem. 89 (24) (2017) 13349–13356.
[32] Z.H. Yang, Y. Zhuo, R. Yuan, Y.Q. Chai, An amplified electrochemical immunosensor based on in situ-produced 1-naphthol as electroactive substance and graphene oxide and Pt nanoparticles functionalized CeO_2 nanocomposites as signal enhancer, Biosens. Bioelectron. 69 (2015) 321–327.
[33] X. Jiao, H. Song, H. Zhao, W. Bai, L. Zhang, Y. Lv, Well-redispersed ceria nanoparticles: promising peroxidase mimetics for H_2O_2 and glucose detection, Anal. Methods. 4 (10) (2012).
[34] T.D. Thanh, J. Balamurugan, S.H. Lee, N.H. Kim, J.H. Lee, Effective seed-assisted synthesis of gold nanoparticles anchored nitrogen-doped graphene for electrochemical detection of glucose and dopamine, Biosens. Bioelectron. 81 (2016) 259–267.
[35] M. Labib, E.H. Sargent, S.O. Kelley, Electrochemical methods for the analysis of clinically relevant biomolecules, Chem. Rev. 116 (16) (2016) 9001–9090.
[36] B. Kong, A. Zhu, Y. Luo, Y. Tian, Y. Yu, G. Shi, Sensitive and selective colorimetric visualization of cerebral dopamine based on double molecular recognition, Angew. Chem. Int. Ed. 50 (8) (2011) 1837–1840.
[37] X. Wang, D. Liu, S. Song, H. Zhang, Pt@CeO_2 multicore@shell self-assembled nanospheres: clean synthesis, structure optimization, and catalytic applications, J. Am. Chem. Soc. 135 (42) (2013) 15864–15872.